Research Article

Multicomponent Equilibrium Isotherms and Kinetics Study of Heavy Metals Removal from Aqueous Solutions Using Electrocoagulation Combined with Mordenite Zeolite and Ultrasonication

Sama Mohammed Al-Jubouri, Rasha Habeeb Salman, Entisar Mohsen Khudhair, Ammar Salih Abbas*, Ahmed Faiq Al-Alawy, Sajad Yas Khudhair, Miqat Hasan Salih and Hassanain Abbas Hassan
Department of Chemical Engineering, College of Engineering, University of Baghdad, Baghdad, Iraq

Abdullatif Alfutimie
Department of Chemical Engineering and Analytical Science, Faculty of Science and Engineering, The University of Manchester, Manchester, United Kingdom

* Corresponding author. E-mail: ammarabbas@coeng.uobaghdad.edu.iq DOI: 10.14416/j.asep.2024.07.011
Received: 17 April 2024; Revised: 21 May 2024; Accepted: 17 June 2024; Published online: 19 July 2024

Abstract
Combining different treatment strategies successively or simultaneously has become recommended to achieve high purification standards for the treated discharged water. The current work focused on combining electrocoagulation, ion-exchange, and ultrasonication treatment approaches for the simultaneous removal of copper, nickel, and zinc ions from water. The removal of the three studied ions was significantly enhanced by increasing the power density (4–10 mA/cm^2) and NaCl salt concentration (0.5–1.5 g/L) at a natural solution pH. The simultaneous removal of these metal ions at 4 mA/cm^2 and 1 g NaCl/L was highly improved by introducing 1 g/L of mordenite zeolite as an ion-exchanger. A remarkable removal of heavy metals was reported, as the initial concentration of each metal decreased from approximately 50 ppm to 1.19 for nickel, 3.06 for zinc, and less than 1 ppm for copper. In contrast, ultrasonication did not show any improvement in the treatment process. The extended Langmuir isotherm model convincingly described the experimental data; the Temkin and Dubinin-Radushkevich isotherm models have proven that the removal processes were physical and exothermic. Finally, the pseudo-second-order kinetics model appropriately explained the kinetics of the process with correlation coefficients of 0.9337 and 0.9016, respectively.

Keywords: Aluminum electrode, Electrocoagulation, Heavy metals, Ion-exchange, Sonication

1 Introduction

Heavy metals in wastewater significantly cause severe toxic impacts on the environment and human health because they are non-biodegradable and extremely toxic even in trace amounts [1]–[5]. Heavy metals are released from the effluents industries such as battery production, metal processing, alloy manufacturing, welding, electroplating, mining, stabilizers, textile, fertilizers, pesticides, petroleum refining, paint, pigment, printing, photographic, and tanneries industries [6], [7]. Heavy metals are commonly classified based on their persistence in the natural environment, causing critical health effects in humans, plants, and animals even at trace levels (1 or 2 μg in some cases). Heavy metals are categorized as macro-nutrient elements, such as cobalt and iron, micro-nutrient elements (e.g., copper, nickel, chromium, iron, manganese, and molybdenum), highly toxic elements (e.g., mercury, cadmium, lead, silver, gold, palladium, bismuth, arsenic, platinum, selenium, tin, and zinc), precious elements (e.g., platinum, silver, gold, palladium, and ruthenium), and radionuclides (e.g., uranium, thorium, radium, cerium, and praseodymium) [8]–[11].

Copper is an essential element for human health because of its ability to support immunity, participate in the generation of leukocytes and erythrocytes, and regularize the endocrine system. However, these benefits are maintained when copper is within the allowable level [12]. Excess copper can lead to stomach discomfort, metabolic disorders, mucosal irritation, necrosis of the liver and kidney, and neurological damage [7]. Due to these severe impacts, the United States World Health Organization and Environmental Protection Agency (US EPA) defined the tolerable level of copper (II) ion in water as 2.0 mg/L and 1.3 mg/L, respectively [8].

Nickel is one of the traditional noxious agents encountered in different industries and released from their effluent to the environment. Therefore, it poses serious problems caused by its carcinogenic potency. Moreover, nickel can adversely influence the implementation of biological treatment processes and the water quality; hence, it constitutes a serious environmental risk [9], [12]. Drinking water exposed to nickel causes weakness, weight gain, and deterioration of the nervous system, lungs, and mucous membranes [13].

Zinc plays a crucial role in regulating life-supporting processes in the digestive and nervous systems and gonad activity influencing pregnancy. Zinc aids wound healing and is responsible for taste perception and visual acuity. However, an excess of zinc can lead to skin breaches, liver disease, weakening of the prostate and the pancreas functions, high blood pressure, and declining immunity [6], [14]. The US EPA established the allowable concentration of nickel and zinc from 0.00003 to 0.8 mg/L [15].

Treatment of wastewater contaminated by heavy metals has been conducted using several technologies such as ion-exchange, adsorption, chemical precipitation, membrane separation, coagulation and flotation, and electrochemical methods [16]–[19]. Electrocoagulation (EC) is a water treatment method based on the electrochemical reaction occurring at the anode when a direct electrical current (DC) is applied across metal electrodes in alkaline pH conditions, which results in hydroxide precipitation, coagulation, and adsorption. These simultaneous approaches work together to remove the dissolved pollutants from wastewater [20], [21]. EC combines the advantages of coagulation, flotation, and electrochemistry [22]. EC is a dependable approach with environmental and economic benefits; therefore, it has been applied in eliminating different pollutants from wastewater effluents, incorporating chemical oxygen demand (COD), oil wastes, and toxic metals [23]. Also, it was reported that EC has achieved successful treatment of galvanic, and/or metal plating wastewater and drinking water [21]. EC allows efficient treatment of pollutants without adding chemicals as only a small weight of sludge is used in simple and small equipment operating over a modest time [24].

Applying a current/voltage between the cathode and anode in the EC approach generates coagulants in the bulk electrolyte solution due to the dissolution of the conductive metal electrode at the anode, which is known as a sacrificial anode (commonly used metals are iron or aluminum) [25]. The water oxidation reaction occurring at the anode leads to the production of oxygen. Simultaneously, another electro-reaction occurs at the cathode between the metal ions and hydroxide ions (OH^-), resulting in hydrogen (H_2) production and water reduction at the cathode [24]. The metal hydroxide precipitates in the electrolytic solution at alkaline pH conditions and works as an adsorbent at pH range 5.5–8.0 to adsorb the pollutants and works as a coagulant at pH above 8 to endorse the coagulation process [20]. Hydrogen gas is liberated from the water in the cathode zone in the form of tiny gas bubbles, which are the basis of the electroflotation (EF) process, allowing the pollutants to be removed from water during the EC process. Accordingly, the EF process makes the EC process perform better to remove the contaminants [26].

The virtual electro-reactions occurring at the electrodes can be explained by Equations (1)–(4) [27].

At the anode:

$$M_{(s)} \leftrightarrow M_{aq}^{n+} + ne^- \quad (1)$$

$$H_2O \rightarrow \left(\frac{1}{2}\right)O_2 + 2H^+ + 2e^- \quad (2)$$

At the cathode:

$$2H_2O + 2e^- \rightarrow 2OH^- + H_2(g) \quad (3)$$

In the bulk electrolyte solution:

$$M_{aq}^{n+} + nOH^- \rightarrow M(OH)_n \quad (4)$$

Where M refers to the electrode metal and n refers to the number of electrons moving in the dissolution process of the anode metal per mole of metal [28].

Assessing many chemical/physical phenomena involved in EC, there are several factors affecting the performance of EC in wastewater treatment that must be considered during application, including alkalinity, conductivity, current density (CD), pH of wastewater, type of wastewater, type of metallic electrodes, electrodes number and size, configuration of metallic electrodes, and operation time [29]–[31]. The CD is a crucial factor in the performance of EC because it affects the production of ions in the cathode and anode and is proportionate with the input voltage. Therefore, ensuring the optimum CD provided in the EC process is important to preserve the lifespan of the electrodes, which is reduced by increasing the CD [31], [32]. The pH of wastewater influences EC's removal process because it is the reason for the formation of different Al species when Al is chemically and electrochemically dissolved. $Al(OH)^{2+}$, $Al(OH)_3$, $Al(OH)_2^+$, $Al_{13}(OH)_{32}^{7+}$, and $Al_2OH_4^{2+}$ having a highly positive surface charge are formed at a pH of 4–9. The active chlorine in the form of hypochlorite appears in high-pH solutions. Compared to hypochlorous acid, this species is a quite weak oxidant toward organic species. Hypochlorous acid is a powerful oxidant and the predominant component in low pH medium [33]. Also, the operation time affects the performance of the EC process because consuming longer time produces more metal ions and hydroxyl on the electrodes [25]. Moreover, water conductivity is important in the EC process because it is established on the electric current. High voltage is required to obtain a typical current intensity for treating low-conductive wastewater. Therefore, it is necessary to add a supporting electrolyte such as sodium chloride (NaCl), potassium chloride (KCl), and sodium nitrate ($NaNO_3$) to treat low-conductive wastewater [34].

Recently, combining different treatment technologies has emerged as a new trend to increase the effectiveness of wastewater treatment. This trend provides a higher removal efficiency to treat polluted effluents compared to a single treatment approach besides their economic viability [35]. A few research has reported combining electrocoagulation with other treatment methods such as coagulation, adsorption, membrane separation, etc. [36]–[39]. Yet, none of the research works is decisive on combining electrocoagulation and ion-exchange processes into a single system for the simultaneous removal of heavy metal ions from aqueous solutions to leverage the benefits of the two processes compared to a single process. Zeolites have been recognized as effective ion-exchangers for heavy metal removal due to the presence of cations occupying the interior structure of zeolites, which allow instantaneous exchange with the positively-charged cations of the polluted metals [40].

Zeolites are microporous minerals consisting of alternations of $[AlO_4]^{5-}$ and $[SiO_4]^{4-}$ tetrahedra, which form the open porous framework of zeolites occupied by cations that balance the negatively charged surface resulting from the existence of Al in the framework [41]. Controlling the aluminum-to-silicon ratio produces various zeolites with ion exchangeability and adjustable channel structure, where the mordenite zeolite (MOR) with a low Si/Al ratio possesses ample complimentary Na^+ because of excesses of negative $[AlO_4]^{5-}$ tetrahedrons [42]. MOR zeolite is a rare natural mineral, whose chemical composition is represented by the chemical formula $Na_8[Al_8Si_{40}O_{96}].24H_2O$, which grants a Si/Al ratio of around 5. However, this ratio changes within a narrow range according to MOR zeolite origin and the generation conditions. Mainly sodium and seldom potassium are the exchangeable cations [43]. Many applications implement zeolites as ion-exchangers, catalysts, adsorbents, and membranes because they have outstanding large surface area, ion-exchange properties, and shape-selectivity [40]. Therefore, MOR zeolite has vastly experienced the removal of multivalent ions due to its powerful ion exchangeability, adequate hydrophilicity, and low expense [42].

Additionally, incorporation of the sonication in the electrocoagulation cell improves the dissolution rate of the Al and Fe anodes and prevents gas bubbles from covering the electrodes, thus promoting the flotation of pollutants. These useful effects of sonication result from its role in improving the movement and hydrodynamics of species. The sonication process encourages the combination of pollutants with coagulants by increasing the mixing efficiency to facilitate the frequency and intensity of collisions between the pollutants and the coagulants [44].

Considering this, the current work studies the potential of adding MOR zeolite to enhance the conditions of the EC process for multicomponent removal. Participation of zeolite in the EC process has been suggested to reduce the treatment time at low electric CD. Zeolite can considerably affect the removal process through its ion-exchange capacity with heavy metal ions; thus, it works together with the adsorbent resulting from the EC process in the removal of multicomponents. Moreover, inducing the zeolite duty in the removal process will be

investigated using ultrasonication. The equilibrium and kinetics models will be studied using different models, namely the extended Langmuir isotherm model, the extended-Langmuir–Freundlich isotherm model, the modified competitive Langmuir isotherm model, pseudo-first-order model, pseudo-second-order model, and intra-particle diffusion model.

2 Experimental Work

2.1 *Materials*

Copper sulphate ($CuSO_4$, 99%, M. Wt. = 159.609) and nickel sulphate-6-hydrate ($NiSO_4.6H_2O$, 99%, M. Wt. = 262.85) were obtained from Sigma. Zinc sulphate heptahydrate ($ZnSO_4.7H_2O$, 99%, M.W. = 287.56) was obtained from Himedia. Sodium chloride (NaCl, 99%, M.W. = 58.44) was obtained from Avonchem. The synthetic MOR zeolite was obtained from a ZR catalyst with a Brunauer, Emmett and Teller (BET) surface area of 400 m^2/g, and Si/Al ratio of 4.17 to 5, and distilled water.

2.2 *Experimental procedures*

The EC experiments were conducted in a batch setup consisting of two electrodes of stainless steel used as cathode with dimensions of 15cm×8cm×3mm for each one with an interspace of 2 cm. The anode was made of aluminum with dimensions of 15cm×8cm× 4mm, and the active area of the two sides of aluminum was 88 cm^2. The anode was fixed in between the two cathodes. Both electrodes were connected to a DC power supply (UNI-T: UTP3315TF-L). The rotation speed was 250 rpm. The glass container was 1 L, containing 0.75 L of the electrolytic solution at room temperature and a constant pH of 7 for all experiments. All chemicals were used as bought with no further treatment. The supporting electrolyte was prepared by dissolving NaCl in distilled water to obtain 0.5, 1, and 1.5 g/L. The electrolyte concentration was studied because it develops the ionic strength, and minimizes the resistance between the electrodes, reduces the formation of the oxide layer on the electrode, minimizes the ion's liberation from the electrodes to the bulk of the polluted solution. The effect of the CD on the removal of the metal ions was studied at 4, 7, and 10 mA/cm^2. The concentration of the metal ions was fixed at 50 mg/L for all experiments, and the removal percentage and the sorption capacity were determined for the metal ions individually and totally.

The effect of adding MOR zeolite on the removal process was studied by adding 1 g/L of MOR zeolite to the metal solution at the lowest CD of 4 mA/cm^2 and NaCl concentration in water, which is 1 g/L. These conditions were selected to investigate the effect of incorporating MOR zeolite and ultrasonication to enhance the removal at low CD conditions and simulated salt concentration in Iraqi waters. All experiments were conducted for 1 h. Also, all concentration readings were the average values obtained from duplicate experiments to obtain an average value of the removal and sorption capacity (q). The electrodes were weighed before and after the experiments. The sludge formed during the electrolysis was separated from the final sample using Whatman filter paper (0.15 μm). Moreover, the added zeolite was separated by filtration at the end of the process to obtain its elemental analysis. The remaining concentration of metal ions was measured by atomic absorption spectrometer model Nov 400, Anlytajena, Germany. Two control experiments were conducted to highlight the effect of participation MOR zeolite in the EC process for multicomponent removal. One experiment was performed using 1 g/L zeolite at 50 mg/L of metal concentration, room temperature, and a constant pH of 7. The second control experiment was conducted using 1 g/L zeolite at 50 mg/L of metal concentration, 1 g/L of NaCl concentration in the solution, room temperature, and pH of 7.

2.3 *Characterization and analysis techniques*

Checking the zeolite phase was carried out by an X-ray diffractometer (XRD) model XRD-6000, Shimadzu, Japan with a radiation source of CuKα of λ = 1.5406 Å, the voltage = 40 kV, the current = 30 mA, a scan speed = 5°/min, a step size = 0.05, and 2θ = 3 to 60°. The morphology of MOR zeolite was characterized by the field emission scanning electron microscope (FESEM) model INSPECT S50, Netherlands. The energy dispersive spectrometer (EDX) used to detect the element type and contents of the samples was carried out by the same FESEM instrument. Ultrasound bath model ISOLAB Laborgerger GmbH, Germany with 60W and 40 kHz inducing the removal process. The value of zero charge point (pHpzc) of MOR zeolite was determined using the solid addition technique in which 0.25 g of MOR zeolite was added to 50 mL of 1 M NaCl solution of different pH 3–13 for 48 h. pHpzc will be obtained by plotting the difference between the final and initial pH readings against the initial reading.

3 Results and Discussion

3.1 *Characterization of MOR zeolite*

Figure 1 shows the XRD pattern of MOR zeolite. The peaks identifying the phase of the used zeolite appeared at 2θ of 13.8°, 19.95°, 22.55°, 25.59°, 26.6°, 27.95°, and 31.2° which are close enough to the reported peaks of MOR zeolite at 2θ of 13.5°, 19.6°, 22.3°, 25.7°, 26.3°, 27.5°, and 30.9° [45], [46]. Also, according to the XRD data and Sherr equation, crystal size was 35.04 nm and crystallinity was 81.31%.

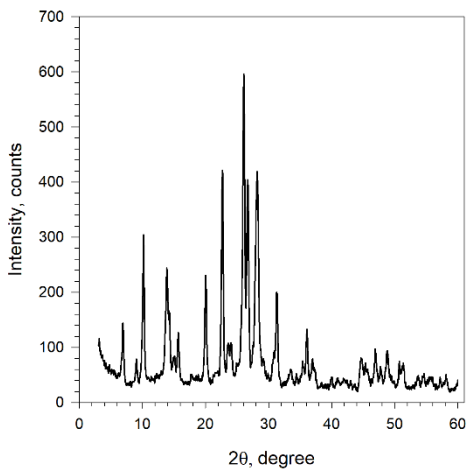

Figure 1: The XRD pattern of MOR zeolite.

Table 1, presenting the EDX results, shows that the Si/Al molar ratio of MOR zeolite before being used in the removal process was 4.78, which is within the range given by the manufacturer. Also, the EDX results show no presence of the elements to be removed in this study. Figure 2 shows the pHpzc of MOR zeolite was about 7.2, impacting the metal ions' removal process.

Table 1: The structural properties of MOR zeolite.

Si wt.%	45.1
Al wt.%	9.42
O wt.%	15.08
Na wt.%	9.89
Si/Al	4.78
Crystal size, nm	35.04
Crystallinity%	81.31
pH_{pzc}	7.2

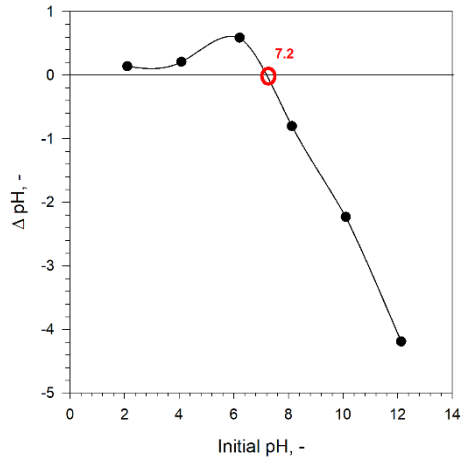

Figure 2: The pH_{pzc} of MOR zeolite.

3.2 *The removal performance*

The experimental results of the removal of metal ions by the EC process are shown in Table 2. Table 2 indicates that increasing the electrolyte concentration and the CD led to an increase in the total removal of the metal ions. This is attributed to the formation of more adsorbent to uptake the metal ions in the bulk solution. At a constant CD, the total removal generally increased by increasing the NaCl concentration in the bulk solution. Also, the total removal generally increased by increasing the CD at a constant NaCl concentration in the bulk solution. Table 2 also shows the voltage decreased with increasing the NaCl concentration at a constant CD. High salt concentration in the bulk solution raises the electrical conductivity and reduces the resistance in the electrolyte solution. Therefore, low voltage was recorded. Table 2 shows that low power consumption was obtained at a constant CD and time. For example, at CD of 7 mA/cm^2, the power was 7145.60 kW/m^3 at 0.5 g NaCl/L; after that, it reduced to 4328.43 kW/m^3 at 1 g NaCl/L, and then it was 3244.27 kW/m^3 at 1 g NaCl/L.

Figure 3 shows that at the same EC experimental conditions, the removal of Cu ions was higher than that of Ni and Zn ions. Also, the removal occurred in a shorter time than for the other metal ions. This can be attributed to the high tendency of Cu ions to be attracted by the adsorbent.

Table 2: The experimental results of the metal ions removal by EC process.

Experiments Conditions	0.5 g/L NaCl			1 g/L NaCl			1.5 g/L NaCl		
	4 mA/cm^2	7 mA/cm^2	10 mA/cm^2	4 mA/cm^2	7 mA/cm^2	10 mA/cm^2	4 mA/cm^2	7 mA/cm^2	10 mA/cm^2
Total removal, %	83.98	95.68	99.36	90.36	98.91	99.72	92.05	99.80	99.83
Average voltage, V	5.02	8.70	13.35	3.16	5.27	5.34	2.85	3.95	4.46
Current, A	0.35	0.62	0.88	0.35	0.62	0.88	0.35	0.62	0.88
Time, h	1	1	1	1	1	1	1	1	1
Power, kW/m^3	2356.05	7145.60	15664.00	1483.09	4328.43	6265.60	1337.60	3244.27	5233.07

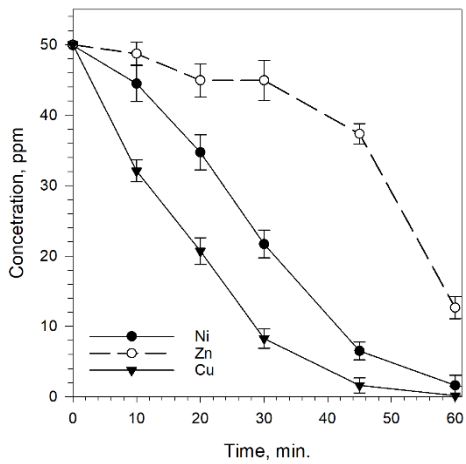

Figure 3: Metal ions removal by EC at 10 mA/cm^2 and 1.5 g NaCl/L.

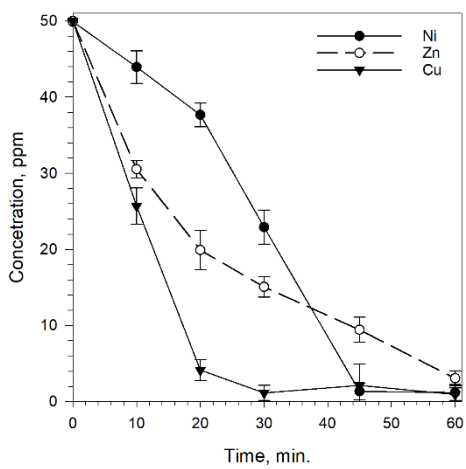

Figure 4: Metal ions removal by EC in the presence of MOR zeolite at 4 mA/cm^2 and 1 g NaCl/L.

The challenge of achieving high ion removal at low power consumption and mimicking Iraqi waters was studied at 4 mA/cm^2 and 1 g NaCl/L in three modes, in the presence of MOR zeolite, under the effect of ultrasonication, and in the presence of MOR zeolite and ultrasonication simultaneously. Figure 4 shows that incorporating MOR zeolite in the EC process was effective as it reduced the remaining concentration of the three metal ions and made the removal process significantly faster. This can be attributed to the ion exchangeability of MOR zeolite due to its content of easily exchangeable cations in its structure, as the EDX result is shown in Table 1. Tiruneh *et al.* [47] reported obtaining a high removal percentage of the studied heavy metals by combining a surplus clay-coagulation process. Table 3 shows the presence of Cu, Ni, and Zn in the elemental analysis of the used MOR zeolite in the removal process.

Additionally, the results of the control experiments presented in Table 4 show that the implementation of the same dose of MOR zeolite alone or in the presence of 1 g/L NaCl to remove 50 mg/L of the multicomponent solution did not achieve the desired goal of removal. The table shows that the presence of electrolyte solution with MOR zeolite did not improve the removal of the metal ions any further. Also, MOR zeolite significantly reduced the concentration of Cu ions from the multicomponent solution, but its performance was weak in the removal of Ni and Zn ions.

Table 3: EDAX results of MOR zeolite after the metal ions removal by EC in the presence of MOR zeolite at 4 mA/cm^2 and 1 g NaCl/L.

Si wt.%	Al wt.%	O wt.%	Na wt.%	Cu wt.%	Ni wt.%	Zn wt.%
58.93	11.79	12.78	5.03	4.78	3.55	3.14

Table 4: The removal of Cu, Ni, and Zn ions using 1 g/L of MOR zeolite alone and in the presence of 1 g NaCl/L after 1 h.

Metal Ions	Removal, % using MOR Zeolite	Removal, % using MOR Zeolite and 1 g/L NaCl
Cu	91.38	89.42
Ni	12.78	12.30
Zn	35.30	34.28

However, introducing the ultrasonic effect on the EC negatively impacted the removal process, especially for Cu^{2+} ions as shown in Figure 5. The incorporation of ultrasonication in the EC process

made it perform less than without ultrasonication. This can be because ultrasonication within the used vibration range worked on the dispersion of the generated adsorbent and prevented enough contact between the metal ions and the adsorbent. This result came against that obtained by Niza *et al.* [48], who reported that the electrocoagulation with vibration-induced electrode plates enhanced the bubble dispersion and ionic transfer in electrocoagulation for pollutant removal. Also, Ozyonar *et al.* [49] reported the positive effect of combining ultrasound irradiation and electrocoagulation treatment because this combination strongly minimized electrode passivation and improved pollutant removal in quicker running times.

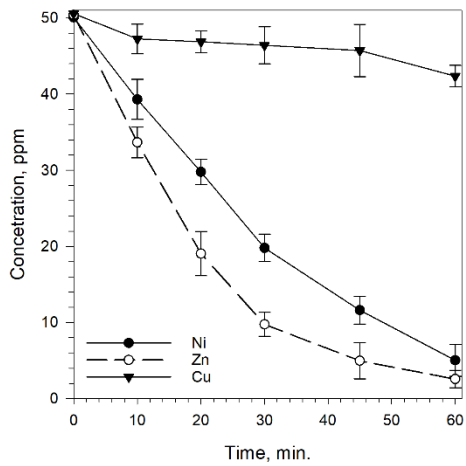

Figure 5: Metal ions removal by EC in the presence of ultrasonication at 4 mA/cm^2 and 1 g NaCl/L.

Figure 6 shows the effect of introducing the ultrasonic impact on the EC in the presence of MOR zeolite to remove the combination of metal ions. On the other side, introducing the ultrasonic effect in the EC process alongside MOR zeolite improved the removal process compared to using the EC and EC combined with ultrasonication. However, it performed less than in the presence of MOR zeolite in the EC process. This result confirms the negative impact of ultrasonication on the dispersion of the adsorbent and the ion-exchanger simultaneously. This impact appeared clearly when a comparison was made among the removal performance of all used modes based on the remaining concentration shown in Figure 7. These results can be attributed to the fact that ultrasonication provides the polluting ions with energy that exceeds the Vander Waals force required for attracting the ions to the adsorbent surface, either the adsorbent generated by EC or MOR zeolite. These findings are consistent with those obtained by Vukojević Medvidović *et al.* [50].

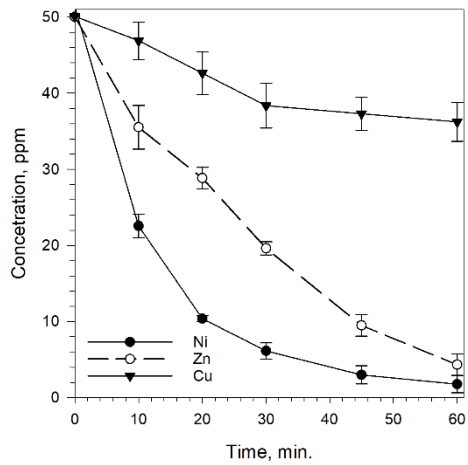

Figure 6: Metal ions removal by EC in the presence of MOR zeolite and ultrasonication at 4 mA/cm^2 and 1 g NaCl/L.

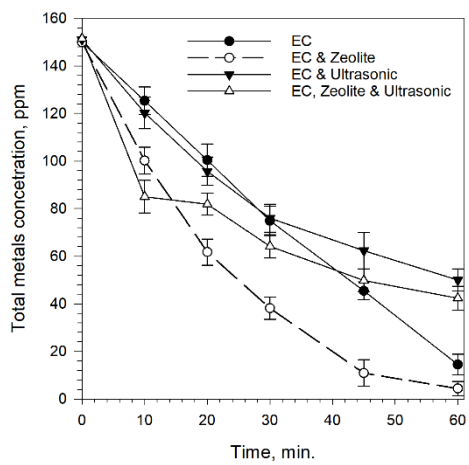

Figure 7: Comparison among the removal modes at 4 mA/cm^2 and 1 g NaCl/L.

3.3 *The isotherm model studies*

Despite being widely used, adsorption isotherm models are black box-type models that do not consider the adsorption mechanism. While these models adequately predict single-component adsorption systems, they fail to capture the complexities of multicomponent systems. The restrictions of multicomponent adsorption models are represented by the inability to predict the competitive and synergistic

effects, i.e., the interactions of various components [51]. Most isotherm models cannot describe the competitive features of multicomponent adsorption systems, like synergistic adsorption, preferential adsorption, and antagonism. Even for similar systems, the model parameters obtained from single-component isotherms systems, e.g., the Langmuir and Freundlich models, are unsuitable for implementation in multicomponent systems.

Furthermore, the heterogeneity of the intrinsic adsorption becomes more difficult when the adsorbent is microporous [52]. The isotherm models, such as the extended Langmuir isotherm model (EL), the Langmuir–Freundlich isotherm model (LF), and the modified competitive Langmuir (MCL) isotherm model are used to fit the obtained experimental results. These models are based on the nonlinear form of the equations, and the prognosis of multicomponent adsorption is prefaced. The maximum adsorption capacity, competitive equilibrium, and affinity parameters can be determined via these models by reducing errors [51]–[54].

The EL isotherm model shown by Equation (5) assumes the adsorbate molecules' uptake on the active sites to have a non-interacting effect. Also, it postulates an equal distribution of adsorption sites and a homogenous surface of adsorbents [55], [56]. However, the isotherm parameters of different adsorbents may show extremely dissimilar values, which is an obstacle to this model [51].

$$q_{eq,i} = q_{max,i} \frac{K_{EL,i}.C_{eq,j}}{1+\sum_{j=1}^{N} K_{EL,i}.C_{eq,j}} \quad (5)$$

Where $q_{eq,i}$ is the equilibrium adsorption capacity (mg/g), $q_{max,i}$ is the maximum adsorption capacity (mg/g), $C_{eq,j}$ is the equilibrium metal ions concentrations (mg/L), and $K_{EL,i}$ is the model constant (L/mg).

The LF isotherm model shown by Equation (6) combines the Freundlich and Langmuir isotherm models to obtain better results by minimizing the limits [57]. The LF isotherm model is generated with all parameters based on multicomponent equilibrium data [51].

$$q_{eq,i} = q_{max,i} \frac{K_{LF,i}.C_{eq,j}^{(1/n_i)}}{1+\sum_{j=1}^{N} K_{LF,i}.C_{eq,j}^{(1/n_i)}} \quad (6)$$

Where $K_{LF,i}$ ((L/mg)–$1/n_i$) is the interaction intensity of adsorbent and adsorbate, and n_i is the favourability and heterogeneity.

The MCL model shown by Equation (7) has the same formula as the EL model but without the interaction factor. The affinity of each component towards the sites and interaction term can be investigated using this model, and the adsorption behavior, such as synergistic/antagonistic, is known based on the interaction coefficient [58].

$$q_{eq,i} = q_{max,i} \frac{K_{MCL,i}.\left(C_{eq,j}/\eta_{MCL,j}\right)}{1+\sum_{j=1}^{N} K_{MCL,i}.\left(C_{eq,j}/\eta_{MCL,j}\right)} \quad (7)$$

Where $K_{EL,i}$ is the model constant (L/mg) and $\eta_{MCL,j}$ is the interaction factor between solutes *i* and *j*.

The correlation coefficients of the studied isotherm models presented in Table 5 show that the EL isotherm model is suitable for describing the experimental data of the removal systems of the Cu, Ni, and Zn ions. This suitability can be attributed to the homogenous surface of adsorbents formed by the EC and the equal distribution of adsorption sites found in MOR zeolite. Table 6 shows the values of q_{max} and the model's constants. Also, the values of $q_{max,1}$ and $q_{max,2}$ were varied and significantly different from the value of $q_{max,3}$.

Table 5: The correlation coefficients of the studied isotherm models.

Process	Isotherm Model		
	EL	LF	MCL
EC	0.9986	0.9829	0.8556
EC + MOR zeolite	0.9337	0.9117	0.7885
EC + Ultrasonication	0.9996	0.9807	0.9674
EC + MOR zeolite + Ultrasonication	0.9994	0.9909	0.9683

Table 6: The EL isotherm model constants for the removal of heavy metals via different processes.

Process	$q_{max,1}$, mg/g	K_1, L/mg	$q_{max,2}$, mg/g	K_2, L/mg	$q_{max,3}$, mg/g	K_3, L/mg
EC	138.94	7.7E-10	111.09	7.2E-10	52.54.3	0.0204
EC + MOR zeolite	84.20	5.7E-5	77.98	1.9E-5	200.9	1.4366
EC + Ultrasonication	153.10	0.2836	102.19	0.1302	26.6	0.0317
EC + MOR zeolite + Ultrasonication	180.81	0.2813	58.60	1.8E-4	63.6	0.0070

Table 7: Temkin and DR isothermal models for the removal of heavy metals via different processes.

	Temkin			DR			
	b, g.J/mol²	**K_T, L/mol**	**R^2, -**	**B, mol²/J²**	**q_s, mol/g**	**E, J/mol**	**R^2, -**
EC	9.7278	0.4072	0.9062	$4*10^{-7}$	4856.14	1118.03	0.8607
EC + MOR zeolite	51.7573	2.1725	0.9061	$3*10^{-8}$	112.98	4082.48	0.7895
EC + Ultrasonication	13.1772	0.1905	0.9045	$8*10^{-7}$	76803.07	790.57	0.8754
EC + MOR zeolite + Ultrasonication	254.6689	$1.5*10^{-5}$	0.9999	$7*10^{-7}$	5865.25	845.15	0.8803

Temkin and Dubinin-Radushkevich (DR) isothermal models were used to determine whether the process is endothermic or exothermic and the type of adsorption (physical or chemical).

The Temkin isotherm can be described by Equation (8) [59].

$$q_e = \frac{RT}{b} \ln K_T + \frac{RT}{b} \ln C_e \quad (8)$$

Where K_T is the equilibrium binding constant (L/mol) corresponding to the maximum binding energy, b is related to the adsorption heat (g.J/mol²), R is the universal gas constant (8.314 J /K.mol), and T is the temperature (K). Plotting q_e versus $\ln(C_e)$ (Equation (8)) results in a straight line of slope RT/b and intercept ($RT \ln K_T$)/b.

The Dubinin-Radushkevich (DR) isotherm model considers that adsorbent size is comparable to the micropore size, and the adsorption equilibrium relation for a given adsorbate-adsorbent combination can be expressed independently of temperature by using the adsorption potential (ε) (Equation (9)).

$$\varepsilon = RT \ln\left(1 + \frac{1}{C_e}\right) \quad (9)$$

The DR isotherm assumes a Gaussian-type distribution for the characteristic curve, and the model can be described by Equation (10).

$$\ln(q_e) = \ln(q_s) - B\varepsilon^2 \quad (10)$$

Where q_s is the DR constant (mol/g), and B gives the mean sorption free energy (E) in J/mol per molecule of sorbate that transfers to the solid surface from the bulk solution and can be computed using Equation (11) [19], [60].

$$E = \frac{1}{(2B)^{1/2}} \quad (11)$$

Values of q_s and B can be determined by linearizing the DR isotherm. Plotting $\ln q_e$ versus ε^2, using Equation (10), results in a straight line of slope B and intercept $\ln(q_s)$.

Table 7 shows the Temkin and DR isothermal model constants.

The values of the heat of adsorption (b values) for all different processes obtained from the Tamkin isotherm model (Equation (8)) are listed in Table 7. The values of adsorption heat were positive for all processes, ranging between 9.7278 and 254.6689 g.J/mol². The positive values of adsorption heat indicate that the adsorption processes for the different studied techniques were endothermic and decreased with the amount of the adsorbed material.

The DR isotherm model (Equations (9)–(11)) was used to calculate the E of the adsorption process for the studied removal techniques. The results (listed in Table 7) showed that E for the EC process was 1118.03 J/mol and increased to 4082.48 J/mol when using the combined process of EC and ion-exchange by the MOR zeolite. In contrast, the results indicated that ultrasonication dramatically reduced the E values.

The results of the two isothermal models (Temkin and DR) indicated that the removal processes were physical due to the significant association of heavy metals (Cu, Ni, and Zn) with the sorbed surface. Also, the released heat became less important during the sorption process, and low values of sorption-free energy were obtained.

3.4 *The kinetic studies*

The combined EC processes involve two or more processes because they have a complicated mechanism of various physiochemical reactions, with adsorption being the main step [61]–[63]. The removal of ions during the combined EC process was due to the role of complex sludge (metal hydroxide) formed during the EC process as an adsorbent and the introduction of MOR zeolite as an ion exchanger. The pseudo-first-order, pseudo-second-order, and intra-particle diffusion models can describe the mechanism of these complex steps in the combined EC process.

Each model has its characteristics, importance, and implications. The pseudo-first-order kinetics model describes the pollutant uptake considering its dependency on the adsorbent capacity, and its kinetics of diffusion is a monolayer. In some adsorption processes, the experimental data of the kinetics do not fit into the pseudo-first-order model over the complete contact time range; however, it can be correctly applied to their initial stages [64]. The linearized form of the pseudo-first-order kinetics model is shown in Equation (12) [62].

$$\ln(q_t - q_{eq}) = \ln q_{eq} + k_1.t \quad (12)$$

Where q_t refers to the mg of metal ions adsorbed by g of adsorbent at time t (min), and k_1 (min^{-1}) is the rate constant of the pseudo-first-order model.

The pseudo-second-order kinetics model indicates that the chemisorption is controlled by the surface adsorption processes relying on solid-phase adsorption in which the occupied sorption sites number is related to the square of the number of unoccupied sorption sites, thus, it is a slow process [64]. The linearized form of the pseudo-second-order kinetics model is shown in Equation (13) [65].

$$\frac{t}{q_t} = \frac{1}{k_2.q_{eq}^2} + \frac{t}{q_{eq}} \quad (13)$$

Where k_2 (mg/g.min) is the rate constant of the pseudo-second-order model.

The intra-particle diffusion kinetics model indicates the involvement of intra-particle diffusion and film diffusion in the sorption process. This model is shown in Equation (14) [50].

$$q_t = k_p.t^{0.5} + C \quad (14)$$

Where k_p (mg/g.$(min)^{0.5}$) is the rate constant of the intra-particle diffusion model and C is a constant related to the film diffusion (mg/g).

Table 8 shows the results of the kinetics study that were obtained. The results indicate that the pseudo-second-order model perfectly described the combined EC process of the heavy metals with acceptable correlation coefficients (0.9016–0.9968). The excellent fit with this kinetics model implies the validation of the assumption that the rate-limiting step is chemisorption, which is caused by valence forces resulting from the sharing or exchange of electrons between metal ions and the adsorbents [64].

4 Conclusions

The current study revealed that introducing MOR zeolite to the EC process resulted in high removal for all three studied heavy metals under low CD and natural salt concentration conditions. However, less promising removal rates were achieved when ultrasonication was introduced to the removal process. Among the three studied metals, copper ions were quickly and highly removed, but their removal became slower when ultrasonication contributed to the removal process. The EL isotherm model successfully described the experimental data with R^2 of 0.9337–0.9996. The removal process was physical and exothermic for the various techniques used, according to the results of Temkin and DR. Additionally, the kinetics of the experiment were appropriately explained by the pseudo-second-order kinetics model with R^2 of 0.9016–0.9968.

Table 8: The results of studying the kinetics models for EC + MOR zeolite.

The model and model's constants		**Ni** ($q_{exp.}$ = 40.8297 mg/g)	**Zn** ($q_{exp.}$ = 39.3791 mg/g)	**Cu** ($q_{exp.}$ = 41.2088 mg/g)
Pseudo-first-order	k_1 (min^{-1})	0.0649	0.0556	0.1182
	q_{eq} (mg/g)	40.8293	39.3777	41.2108
	R^2	0.8807	0.8900	0.7204
Pseudo-second-order	k_2 (mg/g.min)	0.0004	0.0019	0.0032
	q_{eq} (mg/g)	40.8163	39.3701	41.1523
	R^2	0.9901	0.9968	0.9016
Intra-particle diffusion	k_p (mg/g. $(min)^{0.5}$)	8.8031	4.7433	4.0656
	C (mg/g)	25.0360	2.1894	13.7880
	R^2	0.9365	0.9864	0.6410

Author Contributions

S.M.A.: investigation, methodology, writing an original draft, critical revision of the article; R.H.S.: investigation, methodology, data curation, critical revision of the article; E.M.K.: data collection; A.S.A.: research design, data analysis, and interpretation, project administration, critical revision of the article; A.F.A.: investigation, data collection; S.Y.K.: data collection; M.H.S.: data collection; H.A.H.: data collection; A.A.: methodology, drafting the article. All authors have read and agreed to the published version of the manuscript.

Conflicts of Interest

The authors declare no conflict of interest.

References

[1] A. H. Sulaymon, B. A. Abdulmajeed, and A. B. Salman, "Electrochemical removal of cadmium from simulated wastewater using a smooth rotary cylinder electrode," *Desalination and Water Treatment*, vol. 54, no. 9, pp. 2557–2563, 2015, doi: 10.1080/19443994.2014.903520.

[2] A. H. Sulaymon, B. A. Abdulmajeed, and A. B. Salman, "Removal of cadmium from simulated wastewater by using stainless steel concentric tubes electrochemical reactor," *Desalination and Water Treatment*, vol. 68, pp. 220–225, 2017, doi: 10.5004/dwt.2017.20418.

[3] S. M. Al-Jubouri, S. I. Al-Batty, R. Ramsden, J. Tay, S. M. Holmes, and S. M. Al, "Elucidation of the removal of trivalent and divalent heavy metal ions from aqueous solutions using hybrid-porous composite ion-exchangers by nonlinear regression," *Desalination and Water Treatment*, vol. 236, pp. 171–181, 2021, doi: 10.5004/dwt.2021.27707.

[4] P. E. Dim and M. Termtanun, "Treated clay mineral as adsorbent for the removal of heavy metals from aqueous solution," *Applied Science and Engineering Progress*, vol. 14, no. 3, pp. 511–524, 2021, doi: 10.14416/j.asep.2021.04.002.

[5] A. H. Mahvi, B. Davoud, and E. Bazrafshan, "Remarkable reusability of magnetic Fe_3O_4-graphene oxide composite: A highly effective adsorbent for Cr(VI) ions," *International Journal of Environmental Analytical Chemistry*, vol. 103, no. 15, pp. 3501–3521, 2023, doi: 10.1080/03067319.2021.1910250.

[6] I. Ali, A. E. Burakov, A. V. Melezhik, A. V. Babkin, I. V. Burakova, E. A. Neskoromnaya, E. V. Galunin, A. G. Tkachev, and D. V. Kuznetsov, "Removal of copper(ii) and zinc(ii) ions in water on a newly synthesized polyhydroquinone/graphene nanocomposite material: Kinetics, thermodynamics and mechanism," *ChemistrySelect*, vol. 4, no. 43, pp. 12708–12718, Nov. 2019, doi: 10.1002/slct.201902657.

[7] L. Wang, J. Li, J. Wang, X. Guo, X. Wang, J. Choo, and L. Chen, "Green multi-functional monomer based ion imprinted polymers for selective removal of copper ions from aqueous solution," *Journal of Colloid and Interface Science*, vol. 541, pp. 376–386, Apr. 2019, doi: 10.1016/j.jcis.2019.01.081.

[8] K. T. Kubra, M. S. Salman, M. N. Hasan, A. Islam, M. M. Hasan, and M. R. Awual, "Utilizing an alternative composite material for effective copper(II) ion capturing from wastewater," *Journal of Molecular Liquids*, vol. 336, Aug. 2021, Art. no. 116325, doi: 10.1016/j.molliq.2021.116325.

[9] O. A. Oyewo, B. Mutesse, T. Y. Leswifi, and M. S. Onyango, "Highly efficient removal of nickel and cadmium from water using sawdust-derived cellulose nanocrystals," *Journal of Environmental Chemical Engineering*, vol. 7, no. 4, Aug. 2019, Art. no. 103251, doi: 10.1016/j.jece.2019.103251.

[10] S. Rangabhashiyam, R. Jayabalan, M. Asok Rajkumar, and P. Balasubramanian, "Elimination of toxic heavy metals from aqueous systems using potential biosorbents: A review," *Springer Transactions in Civil and Environmental Engineering*, pp. 291–311, Jul. 2018, doi: 10.1007/978-981-13-1202-1_26.

[11] A. Selvi, A. Rajasekar, J. Theerthagiri, A. Ananthaselvam, K. Sathishkumar, J. Madhavan, and P. Rahman, "Integrated remediation processes toward heavy metal removal/recovery from various environments-A review," *Frontiers in Environmental Science*, vol. 7, May 2019, doi: 0.3389/fenvs.2019.00066.

[12] V. G. Georgieva, Lenia Gonsalvesh, and M. P. Tavlieva, "Thermodynamics and kinetics of the removal of nickel (II) ions from aqueous solutions by biochar adsorbent made from agro-waste walnut shells," *Journal of Molecular Liquids*, vol. 312, Aug. 2020, Art. no. 112788, doi: 10.1016/j.molliq.2020.112788.

[13] A. J. Bora and R. K. Dutta, "Removal of metals (Pb, Cd, Cu, Cr, Ni, and Co) from drinking water by oxidation-coagulation-absorption at optimized pH," *Journal of Water Process Engineering*, vol. 31, Oct. 2019, Art. no. 100839, doi:10.1016/ j.jwpe.2019.100839.

[14] A. F. Al-Alawy and M. H. Salih, "Experimental study and mathematical modelling of zinc removal by reverse osmosis membranes," *Iraqi Journal of Chemical and Petroleum Engineering*, vol. 17, pp. 57–73, 2016.

[15] A. Wołowicz and M. Wawrzkiewicz, "Screening of ion exchange resins for Hazardous Ni(ii) removal from aqueous solutions: Kinetic and equilibrium batch adsorption method," *Processes*, vol. 9, no. 2, pp. 285–285, Feb. 2021, doi: 10.3390/pr9020285.

[16] A. B. Salman, "Electrodeposition of lead from simulated wastewater using stainless steel tubes bundle as cathode," *Recent Innovations in Chemical Engineering*, vol. 12, no. 2, pp. 143–159, Sep. 2019, doi: 10.2174/2405520412666190531114218.

[17] R. T. Hadi, A. B. Salman, S. Nabeel, and S. A. Soud, "Recovery of lead from simulated wastewater by using stainless steel rotating cylinder electrode electrochemical reactor," *Desalination and Water Treatment*, vol. 99, pp. 266–271, 2017, doi: 10.5004/dwt.2017.21723.

[18] E. Bazrafshan, M. Sobhanikia, F. K. Mostafapour, H. Kamani, D. Balarak, "Chromium biosorption from aqueous environments by mucilaginous seeds of *Cydonia oblonga*: Thermodynamic, equilibrium and kinetic studies," *Global NEST Journal*, vo. 19, no. 2, pp. 269–277, 2017, doi: 10.30955/gnj.001708.

[19] F. K. Mostafapour, A. H. Mahvi, A. D. Khatibi, M. Khodadadi Saloot, N. Mohammadzadeh, and D. Balarak, "Adsorption of lead(II) using bioadsorbent prepared from immobilized Gracilaria corticata algae: Thermodynamics, kinetics and isotherm analysis," *Desalination and Water Treatment*, vol. 265, pp. 103–113, 2022, doi: 10.5004/dwt.2022.28627.

[20] C. H. Huang, S. Y. Shen, C. D. Dong, M. Kumar, and J. H. Chang, "Removal mechanism and effective current of electrocoagulation for treating wastewater containing Ni(II), Cu(II), and Cr(VI)," *Water*, vol. 12, no. 9, pp. 2614–2614, Sep. 2020, doi: 10.3390/w12092614.

[21] E. Gatsios, J. N. Hahladakis, and E. Gidarakos, "Optimization of electrocoagulation (EC) process for the purification of a real industrial wastewater from toxic metals," *Journal of Environmental Management*, vol. 154, pp. 117–127, May 2015, doi: 10.1016/j.jenvman.2015.02.018.

[22] S. Ayub, A. A. Siddique, M. S. Khursheed, A. Zarei, I. Alam, E. Asgari, and F. Changani, "Removal of heavy metals (Cr, Cu and Zn) from electroplating wastewater by electrocoagulation and adsorption processes," *Desalination and Water Treatment*, vol. 179, pp. 263–271, 2020, doi: 10.5004/dwt.2020.25010.

[23] L. K. Akula, R. K. Oruganti, D. Bhattacharyya, and K. K. Kurilla, "Treatment of marigold flower processing wastewater using a sequential biological-Electrochemical process," *Applied Science and Engineering Progress*, vo. 14, no. 3, pp. 525–542, 2021, doi: 10.14416/j.asep.2021. 04.001.

[24] R. H. Salman, E. M. Khudhair, K. M. Abed, and A. S. Abbas, "Removal of E133 brilliant blue dye from artificial wastewater by electrocoagulation using cans waste as electrodes," *Environmental Progress & Sustainable Energy*, vol. 43, no. 2, Oct. 2023, doi: 10.1002/ep.14292.

[25] R. H. Salman and A. H. Abbar, "Optimization of a combined electrocoagulation-electro-oxidation process for the treatment of Al-Basra Majnoon Oil field wastewater: Adopting a new strategy," *Chemical Engineering and Processing*, vol. 183, Jan. 2023, Art. no. 109227, doi: 10.1016/j.cep. 2022.109227.

[26] F. Ilhan, K. Ulucan-Altuntas, Y. Avsar, U. Kurt, and A. Saral, "Electrocoagulation process for the treatment of metal-plating wastewater: Kinetic modeling and energy consumption," *Frontiers of Environmental Science & Engineering*, vol. 13, no. 5, Sep. 2019, doi: 10.1007/s11783-019-1152-1.

[27] R. H. Salman, "Removal of manganese ions (Mn^{2+}) from a simulated wastewater by electrocoagulation/ electroflotation technologies with stainless steel mesh electrodes: Process optimization based on taguchi approach," *Iraqi Journal of Chemical and Petroleum Engineering*, vol. 20, no. 1, pp. 39–48, Mar. 2019, doi: 10.31699/ijcpe.2019.1.6.

[28] J. N. Hakizimana, B. Gourich, M. Chafi, Y. Stiriba, C. Vial, P. Drogui, and J. Naja, "Electrocoagulation process in water treatment: A review of electrocoagulation modeling approaches," *Desalination*, vol. 404, pp. 1–21, Feb. 2017, doi: 10.1016/j.desal.2016.10.011.

[29] C. An, G. Huang, Y. Yao, and S. Zhao, "Emerging usage of electrocoagulation technology for oil removal from wastewater: A review,"

Science of the Total Environment, vol. 579, pp. 537–556, Feb. 2017, doi: 10.1016/j.scitotenv.2016.11.062.

[30] B. M. Favero, A. C. Favero, D. C. da Silva, P. Hubner, F. S. Souza, and J. B. S. Hamm, "Treatment of galvanic effluent through electrocoagulation process: Cr, Cu, Mn, Ni removal and reuse of sludge generated as inorganic pigment," *Environmental Technology*, vol. 43, pp. 3107–3120, 2022, doi: 10.1080//09593330.2021.1916089.

[31] M. M. Hossain, M. I. Mahmud, M. S. Parvez, and H. M. Cho, "Impact of current density, operating time and ph of textile wastewater treatment by electrocoagulation process," *Environmental Engineering Research*, vol. 18, no. 3, pp. 157–161, Sep. 2013, doi: 10.4491/eer.2013.18.3.157.

[32] M. Nasrullah, N. Islam, and A. W. Zularisam, "Effect of high current density in electrocoagulation process for sewage treatment," *Asian Journal of Chemistry*, vol. 26, no. 14, pp. 4281–4285, Jan. 2014, doi: 10.14233/ajchem.2014.16134.

[33] H. M. Ibrahim and R. H. Salman, "Study the optimization of petroleum refinery wastewater treatment by successive electrocoagulation and electro-oxidation systems," *Iraqi Journal of Chemical and Petroleum Engineering*, vol. 23, no. 1, pp. 31–41, Mar. 2022, doi: 10.31699/ijcpe.2022.1.5.

[34] E. Keshmirizadeh, S. Yousefi, and M. K. Rofouei, "An investigation on the new operational parameter effective in Cr(VI) removal efficiency: A study on electrocoagulation by alternating pulse current," *Journal of Hazardous Materials*, vol. 190, no. 1–3, pp. 119–124, Jun. 2011, doi: 10.1016/j.jhazmat.2011.03.010.

[35] F. Hussin, M. Aroua, and M. Szlachta, "Combined solar electrocoagulation and adsorption processes for Pb(II) removal from aqueous solution," *Chemical Engineering and Processing*, vol. 143, Sep. 2019, Art. no. 107619, doi: 10.1016/j.cep.2019.107619.

[36] N. S. Graça and A. E. Rodrigues, "The combined implementation of electrocoagulation and adsorption processes for the treatment of wastewaters," *Clean Technologies*, vol. 4, no. 4, pp. 1020–1053, Oct. 2022, doi: 10.3390/cleantechnol4040063.

[37] E. Bazrafshan, M. R. Alipour, and A. H. Mahvi, "Textile wastewater treatment by application of combined chemical coagulation, electrocoagulation, and adsorption processes," *Desalination and Water Treatment*, vol. 57, pp. 9203–9215, 2016, doi: 10.1080//19443994.2015.1027960.

[38] Y. Dehghani, B. Honarvar, A. Azhdarpour, and M. Nabipour, "Treatment of wastewater by a combined technique of adsorption, electrocoagulation followed by membrane separation," *Advances in Environmental Technology*, vol. 7, no. 3, pp. 171–183, Aug. 2021, doi: 10.22104/aet.2021.5133.1394.

[39] A. Aouni, R. Lafi, and A. Hafiane, "Feasibility evaluation of combined electrocoagulation/adsorption process by optimizing operating parameters removal for textile wastewater treatment," *Desalination Water Treatment*, vol. 60, pp. 78–87, 2017, doi: 10.5004/dwt.2017.10890.

[40] S. M. Al-Jubouri, S. I. Al-Batty, S. Senthilnathan, N. Sihanonth, L. Sanglura, H. Shan, and S. M. Holmes, "Utilizing Faujasite-type zeolites prepared from waste aluminium foil for competitive ion-exchange to remove heavy metals from simulated wastewater," *Desalination Water Treatment*, vol. 231, pp. 166–181, 2021, doi: 10.5004/dwt.2021.27461.

[41] H. N. Alfalahy and S. M. Al-Jubouri, "Preparation and application of polyethersulfone ultrafiltration membrane incorporating NaX zeolite for lead ions removal from aqueous solutions," *Desalination Water Treatment*, vol. 248, pp. 149–162, 2022, doi: 10.5004/dwt.2022.28072.

[42] P. Nie, B. Hu, X. Shang, Z. Xie, M. Huang, and J. Liu, "Highly efficient water softening by mordenite modified cathode in asymmetric capacitive deionization," *Separation and Purification Technology*, vol. 250, Nov. 2020, Art. no. 117240, doi: 10.1016/j.seppur.2020.117240.

[43] K. M. Wojciechowska, M. Król, T. Bajda, and W. Mozgawa, "Sorption of heavy metal cations on mesoporous ZSM-5 and mordenite zeolites," *Materials*, vol. 12, no. 19, pp. 3271–3271, Oct. 2019, doi: 10.3390/ma12193271.

[44] P. Asaithambi, A. Raman, B. Sajjadi, and W. Mohd, "Sono assisted electrocoagulation process for the removal of pollutant from pulp and paper industry effluent," *Environmental Science and Pollution Research International*, vol. 24, no. 6, pp. 5168–5178, May 2016, doi: 10.1007/s11356-016-6909-5.

[45] H. M. Lankapati, D. R. Lathiya, L. Choudhary, A. K. Dalai, and K. C. Maheria, "Mordenite-type zeolite from waste coal fly ash: Synthesis, characterization and its application as a sorbent

in metal ions removal," *ChemistrySelect*, vol. 5, no. 3, pp. 1193–1198, Jan. 2020, doi: 10.1002/slct.201903715.

[46] P. Intarapong, S. Iangthanarat, and P. Phanthong, "Activity and basic properties of KOH/mordenite for transesterification of palm oil," *Journal of Energy Chemistry*, vol. 22, no. 5, p. 690, Sep. 2013.

[47] A. T. Tiruneh, T. Y. Debessai, G. C. Bwembya, and S. J. Nkambule, "Combined clay adsorption-coagulation process for the removal of some heavy metals from water and wastewater," *American Journal of Environmental Engineering*, vol. 8, no. 2, pp. 25–35, 2018, doi: 10.5923/j.ajee.20180802.02.

[48] N. M. Niza, M. S. Yusoff, M. A. A. Mohd Zainuri, M. I. Emmanuel, A. M. H. Shadi, and M. A. Kamaruddin, "Performance of batch electrocoagulation with vibration-induced electrode plates for landfill leachate treatment," *Journal of Water Process Engineering*, vol. 36, Aug. 2020, Art. no. 101282, doi: 10.1016/j.jwpe.2020.101282.

[49] F. Özyonar, Ö. Gökkuş, M. Sabuni, "Removal of disperse and reactive dyes from aqueous solutions using ultrasound-assisted electrocoagulation," *Chemosphere*, vol. 258, Nov. 2020, Art. no. 127325, doi: 10.1016/j.chemosphere.2020.127325.

[50] N. V. Medvidović, L. Vrsalović, S. Svilović, and M. Cestarić, "Comparison of electrocogulation couples with synthetic zeolite, ultrasound and two steps electrocogulation," *Journal of Sustainable Technologies and Materials*, vol. 2, no. 3, pp. 1–10, Dec. 2022, doi: 10.57131/jstm.2022.3.1.

[51] N. Amrutha, G. Jeppu, C. R. Girish, B. Prabhu, and K. Mayer, "Multi-component adsorption isotherms: Review and modeling studies," *Environmental Processes*, vol. 10, no. 2, Jun. 2023, doi: 10.1007/s40710-023-00631-0.

[52] A. J. Jadhav and V. C. Srivastava, "Multicomponent adsorption isotherm modeling using thermodynamically inconsistent and consistent models," *AIChE Journal*, vol. 65, no. 11, Jul. 2019, doi:10.1002/aic.16727.

[53] F. K. Al-Jubory, A. S. Abbas, and I. M. Mujtaba, "Adsorptive removal of ciprofloxacin from simulated wastewater using crosslinked starch ester: Isotherms, kinetics, thermodynamics, modeling, and simulation for continuous operation," *Chemical Engineering Research & Design*, vol. 200, pp. 332–343, Dec. 2023, doi: 10.1016/j.cherd.2023.10.051.

[54] S. Barno and A. S. Abbas, "Reduction of organics in dairy wastewater by adsorption on a prepared charcoal from iraqi sugarcane," *IOP Conference Series. Materials Science and Engineering*, vol. 736, no. 2, Jan. 2020, Art. no. 022096, doi: 10.1088/1757-899x/736/2/022096.

[55] S. Sohn and D. Kim, "Modification of Langmuir isotherm in solution systems—definition and utilization of concentration dependent factor," *Chemosphere*, vol. 58, no. 1, pp. 115–123, Jan. 2005, doi: 10.1016/j.chemosphere.2004.08.091.

[56] S. K. Pereira, S. Kini, B. Prabhu, and G. P. Jeppu, "A simplified modeling procedure for adsorption at varying pH conditions using the modified Langmuir–Freundlich isotherm," *Applied Water Science*, vol. 13, no. 1, Dec. 2022, doi: 10.1007/s13201-022-01800-6.

[57] C. Stefanne, B. Galdeano, R. Landers, Carlos, and M. Gurgel, "Equilibrium study of binary mixture biosorption of Cr(III) and Zn(II) by dealginated seaweed waste: Investigation of adsorption mechanisms using X-ray photoelectron spectroscopy analysis," *Environmental Science and Pollution Research International*, vol. 26, no. 28, Aug. 2018, Art. no. 28480, doi: 10.1007/s11356-018-2880-7.

[58] V. C. Srivastava, I. D. Mall, and I. M. Mishra, "Removal of cadmium(II) and zinc(II) metal ions from binary aqueous solution by rice husk ash," *Colloids and Surfaces. A, Physicochemical and Engineering Aspects*, vol. 312, no. 2–3, pp. 172–184, Jan. 2008, doi: 10.1016/j.colsurfa.2007.06.048.

[59] A. Alameri, R. Alfilh, S. Awad, G. Zaman, T. J. Al-Musawi, M. Joybari, D. Balarak, and McKay, "Ciprofloxacin adsorption using magnetic and ZnO nanoparticles supported activated carbon derived from Azolla filiculoides biomass," *Biomass Conversion and Biorefinery*, Oct. 2022, doi: 10.1007/s13399-022-03372-6.

[60] R. K. Abid and A. S. Abbas, "Adsorption of organic pollutants from real refinery wastewater on prepared cross-linked starch by epichlorohydrin," *Data in Brief*, vol. 19, pp. 1318–1326, Aug. 2018, doi: 10.1016/j.dib.2018.05.060.

[61] Z. Al-Qodah, M. Tawalbeh, M. Al-Shannag, Z. Al-Anber, and K. Bani-Melhem, "Combined electrocoagulation processes as a novel approach for enhanced pollutants removal: A state-of-the-art review," *Science of the Total Environment*,

vol. 744, Nov. 2020, Art. no. 140806, doi: 10.1016/j.scitotenv.2020.140806.

[62] S. U. Khan, M. Khalid, K. Hashim, M. H. Jamadi, M. Mousazadeh, F. Basheer, and I. H. Farooqi, "Efficacy of electrocoagulation treatment for the abatement of heavy metals: An overview of critical processing factors, kinetic models and cost analysis," *Sustainability*, vol. 15, no. 2, pp. 1708–1708, Jan. 2023, doi: 10.3390/su15021708.

[63] A. S. Abbas and S. A. Hussien, "Equilibrium, kinetic and thermodynamic study of aniline adsorption over prepared ZSM-5 zeolite," *Iraqi Journal of Chemical and Petroleum Engineering*, vol. 18, no. 1, pp. 47–56, Mar. 2017, doi: 10.31699/ijcpe.2017.1.4.

[64] M. Ghahrchi, A. Rezaee, and A. Adibzadeh, "Study of kinetic models of olive oil mill wastewater treatment using electrocoagulation process," *Desalination and Water Treatment*, vol. 211, pp. 123–130, 2021, doi: 10.5004/dwt.2021.26516.

[65] A. A. Moneer, N. M. El-Mallah, M. M. El-Sadaawy, M. Khedawy, and M. S. H. Ramadan, "Parameters optimization, kinetics, isotherm modeling of cationic and disperse dyes removal procedure using bi-polar iron electrocoagulation system," *Desalination and Water Treatment*, vol. 256, pp. 300–313, 2022, doi: 10.5004/dwt. 2022.28416.